Journal of Pharmaceutical and Biomedical Analysis 177 (2020) 112851

Contents lists available at ScienceDirect

Journal of Pharmaceutical and Biomedical Analysis

journal homepage: www.elsevier.com/locate/jpba

Simultaneous determination of chiral and achiral impurities of ivabradine on a cellulose tris(3-chloro-4-methylphenylcarbamate) chiral column using polar organic mode

Elek Ferencz[a,b], Béla Kovács[a,b], Francisc Boda[a], Mohammadhassan Foroughbakhshfasaei[c], Éva Katalin Kelemen[b], Gergő Tóth[c,*], Zoltán-István Szabó[a,b,**]

[a] Faculty of Pharmacy, University of Medicine, Pharmacy, Sciences and Technology of Targu Mures, Gh. Marinescu 38, RO-540139, Tîrgu Mureş, Romania
[b] Gedeon Richter Romania S.A., RO-540306, Tîrgu Mureş, Romania
[c] Department of Pharmaceutical Chemistry, Semmelweis University, Hőgyes E. u. 9, Budapest, Hungary

ARTICLE INFO

Article history:
Received 14 June 2019
Received in revised form 29 August 2019
Accepted 30 August 2019
Available online 30 August 2019

Keywords:
Chemoselectivity
Polar organic mode
Chiral separation
Related substance
HPLC

ABSTRACT

A high performance liquid chromatographic method was developed for the simultaneous determination of the related substances (*R*-ivabradine, dehydro-*S*-ivabradine, *N*-demethyl-*S*-ivabradine, ((*S*)-3,4-dimethoxy-bicyclo[4.2.0]octa-1,3,5-triene-7-yl-methyl)-methyl-amine) and 1-(7,8-dimethoxy-1,3,4,5-tetrahydro-2*H*-3-benzazepine-2-on-3-yl)-3-chloro-propane) of the heart-rate lowering drug, ivabradine. The separation capability of seven different polysaccharide-type chiral columns (Lux Amylose-1, Lux i-Amylose-1, Lux Amylose-2, Lux Cellulose-1, Lux Cellulose-2, Lux Cellulose-3 and Lux Cellulose-4) was investigated with a mobile phase consisting of 0.1% diethylamine in methanol, 2-propanol and acetonitrile. During the screnning experiments the best results were obtained on Lux Cellulose-2 (based on cellulose tris(3-chloro-4-methylphenylcarbamate) column with methanol with an ideal case, where all the impurities eluted before the *S*-ivabradine peak. Chromatographic parameters (flow rate, temperature and mobile phase constituents) were optimized by a full factorial screening design. Using optimized parameters (Lux Cellulose-2 column with 0.06% (v/v) diethylamine in methanol/acetonitrile 98/2 (v/v) with 0.45 mL/min flow rate at 12 °C) baseline separations were achieved between all compounds. The optimized method was validated according to the International Council on Harmonization Q2(R1) guideline and proved to be reliable, linear, precise and accurate for determination of at least 0.05% for all impurities in *S*-ivabradine samples. Method application was tested on a commercial tablet formulation and proved to be suitable for routine quality control of both chiral and achiral related substances of *S*-ivabradine.

© 2019 The Authors. Published by Elsevier B.V. This is an open access article under the CC BY-NC-ND license (http://creativecommons.org/licenses/by-nc-nd/4.0/).

1. Introduction

Ivabradine 3-{3-[((*S*)-3,4-dimethoxy-bicyclo[4.2.0]octa-1,3,5-triene-7-ylmethyl)-methyl-amino]-propyl}-7,8-dimethoxy-1,3,4,5-tetrahydro-2*H*-3-benzazepine-2-one; IVA) is an orally bioavailable, hyperpolarization-activated, cyclic nucleotide-gated channel inhibitor. It is used for chronic heart failure not fully managed by β-blockers [1,2]. IVA has a single asymmetric carbon atom, resulting in two optical isomers. The drug is marketed as a single enantiomeric agent; the pharmaceutical formulations contain only the *S*-enantiomer, because of its improved electrophysiological selectivity [3,4]. Nevertheless, to date, only one application note from Daicel Chiral technologies is available for chiral separation of IVA using Chiralpak IG (based on amylose tris(3-chloro-5-methylphenylcarbamate) column [5]. Moreover, the number of the described method for determination of achiral related substances in IVA is also limited [6–9]. High performance liquid chromatography (HPLC) using a chiral stationary phase (CSP) is the golden standard in analytical enantioseparation due to the several advantages it offers, such as ease of use, robustness and

* Corresponding author at: Department of Pharmaceutical Chemistry, Semmelweis University, H-1092 Budapest, Hőgyes E. u. 9, Hungary.
** Corresponding author at: Faculty of Pharmacy, University of Medicine, Pharmacy, Sciences and Technology of Targu Mures, Gh. Marinescu 38, Gedeon Richter Romania S.A., RO-540306, Tîrgu Mureş, Romania.
E-mail addresses: toth.gergo@pharma.semmelweis-univ.hu (G. Tóth), zoltan.szabo@gedeon-richter.ro, zoltan.szabo@umfst.ro (Z.-I. Szabó).

https://doi.org/10.1016/j.jpba.2019.112851
0731-7085/© 2019 The Authors. Published by Elsevier B.V. This is an open access article under the CC BY-NC-ND license (http://creativecommons.org/licenses/by-nc-nd/4.0/).

good transferability between laboratories. Today, out of numerous CSPs available on the market, polysaccharide-type CSPs are the most frequently applied, due to their high enantiorecognition capability for most of the compounds and multimodal nature [10–12]. These columns can be operated in normal phase, reversed phase and polar organic mobile phase modes. In polar organic mode only polar organic solvents, neat alcohols (methanol, ethanol and 2-propanol), neat acetonitrile (ACN) or their combinations are used as mobile phase. Polar organic mode has several advantages, such as shorter run times, high efficiency, and usually higher solubility of the analytes in the mobile phase [12–15]. Apart from their ability to discriminate between enantiomers, polysaccharide-type CSPs may also present excellent chemoselectivity for structurally related compounds, therefore they can be used for simultaneous determination of chiral and chemical impurities [14,16,17].

All specified impurities, including *R*-enantiomer are of interest in the analysis of *S*-IVA. Therefore, the aim of the present study was to develop a method for the simultaneous determination of *R*-IVA, dehydro-*S*-ivabradine (DHIVA), *N*-demethyl-*S*-ivabradine (DMIVA), ((*S*)-3,4-dimethoxy-bicyclo[4.2.0]octa-1,3,5-triene-7-yl-methyl)-methyl-amine (IMP-1) and 1-(7,8-dimethoxy-1,3,4,5-tetrahydro-2*H*-3-benzazepine-2-on-3-yl)-3-chloro-propane (IMP-2) (Fig. 1) in *S*-IVA samples with a limit of quantification of at least 0.05% or below.

2. Materials and methods

2.1. Materials

S-IVA (as a hydrobromide salt), racemic IVA, *N*-demethyl-*S*-ivabradine (DMIVA, 3-{3-[((*S*)-3,4-dimethoxy-bicyclo[4.2.0]octa-1,3,5-triene-7-yl)-methyl-amino]-propyl}-7,8-dimethoxy-1,3,4,5-tetrahydro-2H-3-benzazepine-2-one), dehydro-*S*-ivabradine (DHIVA, 3-{3-[((*S*)-3,4-dimethoxy-bicyclo[4.2.0]octa-1,3,5-triene-7-ylmethyl)-methyl-amino]-propyl}-7,8-dimethoxy-1,3-dihydro-2*H*-3-benzazepine-2-one), ((*S*)-3,4-dimethoxy-bicyclo[4.2.0]octa-1,3,5-triene-7-yl-methyl)-methyl-amine (IMP-1) and 1-(7,8-dimethoxy-1,3,4,5-tetrahydro-2*H*-3-benzazepine-2-on-3-yl)-3-chloro-propane (IMP-2) (Fig. 1) were obtained from a pharmaceutical company in Târgu Mureş. Diethylamine (DEA) ≥99.5% was purchased from Sigma-Aldrich (Budapest, Hungary). Gradient grade methanol (MeOH), 2-propanol (IPA) and acetonitrile (ACN) were purchased from Thomasker Finechemicals Ltd. (Budapest, Hungary).

Ultrapure, deionized water was prepared by a Milli-Q Direct 8 Millipore system (Milford, MA, USA). *S*-IVA 5 mg film-coated tablets were obtained from Central Pharmacy of Semmelweis University (Budapest, Hungary). All chiral columns with identical dimensions (4.6 x 150 mm, 5 μm particles) were ordered from Phenomenex (Torrance, CA, USA): Lux Cellulose-1 [cellulose tris(3,5-dimethylphenylcarbamate)], Lux Cellulose-2 [cellulose tris(3-chloro-4-methylphenylcarbamate)], Lux Cellulose-3 [cellulose tris(4-methylbenzoate)], Lux Cellulose-4 [cellulose tris(4-chloro-3-methylphenylcarbamate)], Lux Amylose-1 [amylose tris(3,5-dimethylphenylcarbamate)], Lux i-Amylose-1 [amylose tris(3,5-dimethylphenylcarbamate)], immobilized and Lux Amylose-2 [amylose tris(5-chloro-2-methylphenylcarbamate)] (Supplementary Information Figure S1).

2.2. LC-UV analysis

LC-UV experiments was carried out on a JASCO HPLC system (JASCO PU-2089 Plus binary gradient pump, AS-4050 autosampler, MD-2010 Plus diode array detector and CO2065 Plus column oven). The software used to operate the equipment and data processing was ChromNAV. UV detection was performed at 286 nm. MeOH was used as a sample solvent for the preparation of solutions throughout the study. For the preliminary experiments, stock solutions of 200 μg/mL *S*-IVA were prepared in MeOH and were spiked with impurities at around 2% (around 4 μg/mL). The final test solution of *S*-IVA used for validation and method applicability testing was about 8000 μg/ml. All impurity level percentages are reported relative to this concentration. An injection volume of 5 μL was used and three parallel measurements were performed in all cases.

For preparation of sample solutions, ten tablets were weighted, then ground and mixed in a mortar. In a 5 mL volumetric flask, MeOH was added to an accurately weighted portion of the tablet powder corresponding to about 40 mg *S*-IVA. Then the suspension was sonicated for 30 min and centrifuged for 2 min applying 4000 rpm (Sartorius 2–16 P benchtop centrifuge, Goettingen, Germany). The clear supernatant was filtered through 0.22 μm pore size syringe containing PVDF filter (FilterBio membrane Co., LTD, Nantong City, China).

The experimental design and multivariate method optimization was performed with the aid of Modde 11 software (Umetrics, Sweden).

3. Results and discussion

3.1. Method scouting phase

In routine quality control of single enantiomeric pharmaceutical substances, the “classical approach” would be to develop separate methods for the quantification of achiral and chiral related substances. Methods that enable simultaneous quantification of both chiral and achiral impurities are thus highly welcome, because they can significantly shorten the analysis time. However, in these cases, the developed methods need to display both enantioselectivity (chiral separation) and chemoselectivity (achiral separation) towards the analytes. Although this can also be achieved by tandem coupling of chiral and achiral columns, using a single chiral column is more desirable. Thus, for the present method, based on regulatory considerations, the analytical target profile was defined as a method that would allow the precise and accurate determination of all selected impurities (chiral and chemical) at a level of at least 0.05% or below, in short analysis time ($t \leq 30$ min).

Recently, we have successfully applied polysaccharide-based CSPs in polar organic mode for the chiral separation of a large variety of analytes [18–21], however polysaccharide-type CSPs have also proved their capability for simultaneous chiral-achiral analyses [14,16,17].

Polysaccharide-based CSPs come in a wide variety of commercially available columns and usually display a great variety of enantio- and chemoselectivity. In the present study, seven different polysaccharide-based CSPs, including amylose-based Lux Amylose-1, Lux i-Amylose-1 and Lux Amylose-2, as well as cellulose-based Lux Cellulose-1, Lux Cellulose-2, Lux Cellulose-3 and Lux Cellulose-4 were tested in polar organic mode using a mobile phase consisting of 0.1% DEA in MeOH, IPA or ACN, with 0.5 mL/min flow rate at 25 °. In our screening the combination of polar organic solvents was not used, however it should be noted that solvent mixture can change the enantiorecognition mechanism and also can improve the resolution.

During the screening step in all cases, IMP-1 and IMP-2 were well resolved from each other and the main peak, however, difficulties were observed during the separation of the structurally very similar DHIVA, DMIVA, *R*-IVA from the main peak for which co-elutions were often observed. Particularly challenging was the resolution of IVA enantiomers, which was identified as the critical

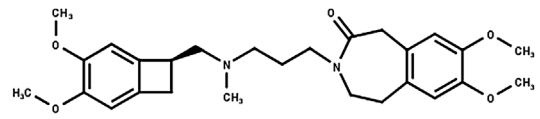

***S*-ivabradine**

IVA

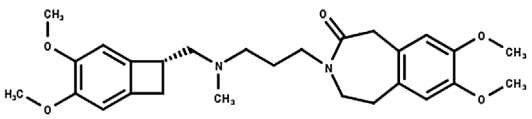

***R*-ivabradine**

***R*-IVA**

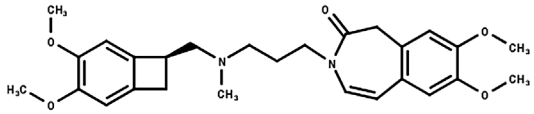

dehydro-*S*-ivabradine

DHIVA

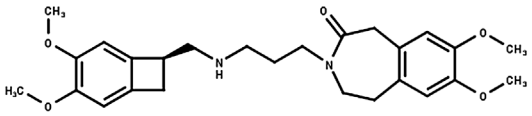

N-demethyl-*S*-ivabradine

DMIVA

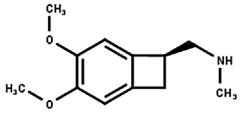

((*S*)-3,4-dimethoxy-bicyclo[4.2.0]octa-1,3,5-triene-7-yl-methyl)-methyl-amine

IMP-1

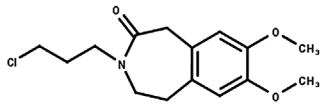

1-(7,8-dimethoxy-1,3,4,5-tetrahydro-2H-3-benzazepine-2-on-3-yl)-3-chloro-propane

IMP-2

Fig. 1. Name, chemical structure and abbreviations of the compounds used in this study.

Table 1
Summary of the chromatographic data obtained during the preliminary screening phase.

Column	Mobile phase*	R_s	Enantiomer elution order	t_r, min	Last eluted compound
	MeOH	0.25	R < S	23.1	*S*-IVA
Lux Amylose-1	IPA	1.34	R < S	16.1	*S*-IVA
	ACN	0.24	S < R	19.0	DMIVA
	MeOH	–	–	11.2	IVA
Lux i-Amylose-1	IPA	0.86	R < S	20.3	*S*-IVA
	ACN	–	–	10.8	IVA
	MeOH	1.06	S < R	18.2	*R*-IVA
Lux Amylose-2	IPA	–	–	49.3	DMIVA
	ACN	1.80	S < R	49.9	DMIVA
	MeOH	2.15	S < R	10.6	*R*-IVA
Lux Cellulose-1	IPA	1.64	S < R	19.6	DMIVA
	ACN	2.60	S < R	8.9	DMIVA
	MeOH	1.78	R < S	19.9	*S*-IVA
Lux Cellulose-2	IPA	–	–	40.9	DMIVA
	ACN	0.20	R < S	39.3	DMIVA
	MeOH	2.73	S < R	9.3	*R*-IVA
Lux Cellulose-3	IPA	–	–	11.7	DMIVA
	ACN	–	–	5.0	DMIVA
	MeOH	0.25	R < S	14.1	*S*-IVA
Lux Cellulose-4	IPA	–	–	35.8	DMIVA
	ACN	1.11	R < S	26.4	DMIVA

R_s, resolution between *R*- and *S*-IVA.
t_r, retention time of the last eluted peak.
* all mobile phases contained 0.1% DEA as basic modifier.
- no enantiorecognition could be observed.

parameter. Thus, the screening was focused mainly on selecting the adequate column for baseline separation of the enantiomers with the desired elution order (chiral impurity and *R*-IVA eluting before the eutomer). Some of the chromatograms obtained are depicted in Fig. 2, while the relevant chromatographic data are presented in Table 1. As it can be observed, baseline chiral separation between

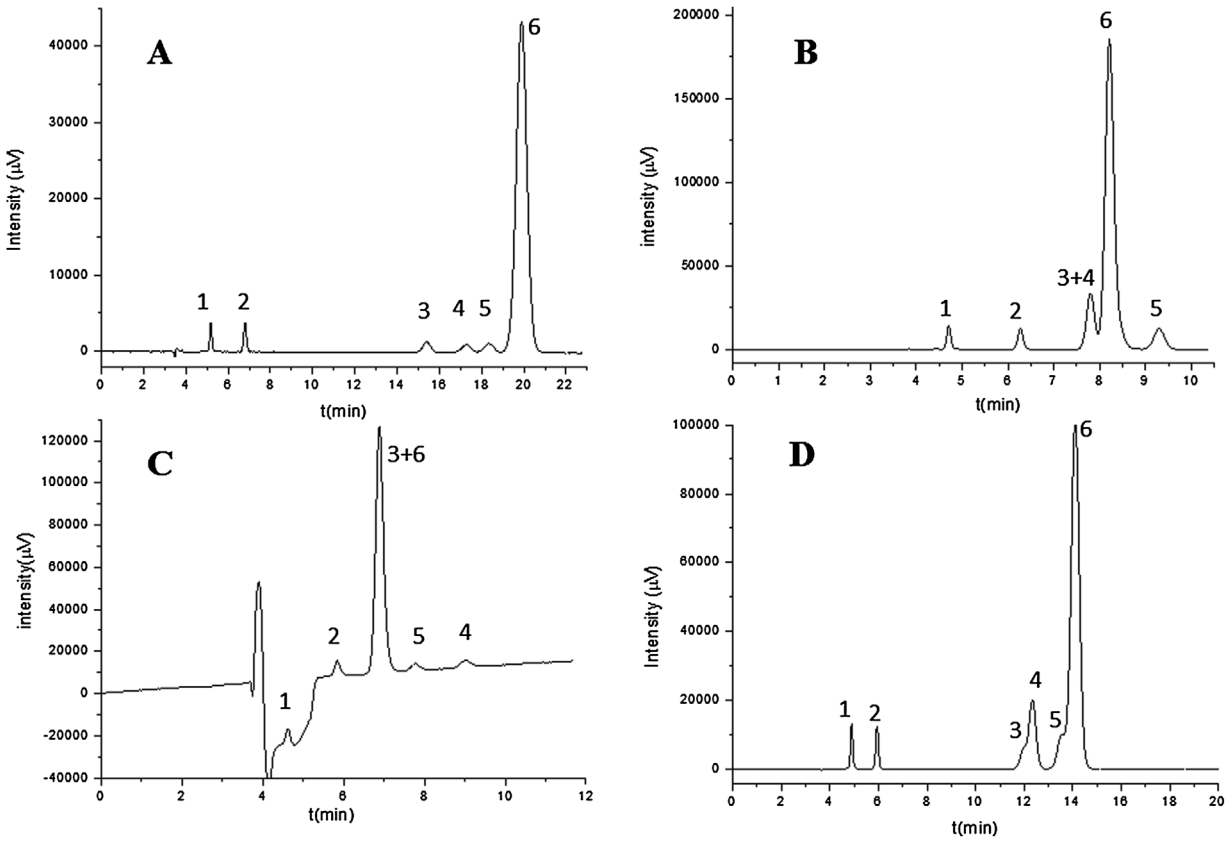

Fig. 2. Representative chromatograms obtained during the preliminary study. Chromatographic conditions: (A) Lux Cellulose-2 with 0.1% DEA in MeOH; (B) Lux Cellulose-3 with 0.1% DEA in MeOH; (C) Lux Cellulose-2 with 0.1% DEA in ACN; (D) Lux Cellulose-4 with 0.1% DEA in MeOH (flow rate: 0.5 mL/min, temperature 25 °C, detection at 286 nm.) 1. IMP-1, 2. IMP-2, 3. DHIVA, 4. DMIVA, 5. *R*-IVA, 6. *S*-IVA.

enantiomers was achieved on the Lux Cellulose-1 column with high resolution values for all three mobile phases, but the elution order of the enantiomers was unfavorable. Distomer-first elution order was observed on Lux-i-Amylose-1, Lux Cellulose-2 and Lux Cellulose-4, but the baseline separation was achieved only in the case of Lux Cellulose-2 using 0.1% DEA in MeOH as mobile phase. Mobile phase dependent enantiomer elution order was recorded on Lux Amylose-1 column, when changing the main component of the mobile phase from alcohols to ACN.

Since the final goal was to develop a single method for the separation of all related substances, not only enantioselectivity, but chemoselectivity was also important. Thus, for further method optimization the following starting-point was selected: Lux Cellulose-2 column, with 0.1% DEA in MeOH with 0.5 mL/min flow rate at 25 °C. By applying this method, all investigated related substances could be resolved. Moreover, not only the enantiomeric impurity *R*-IVA, but all investigated impurities eluted before *S*-IVA (Fig. 2A). In an attempt to gain higher resolution MeOH was changed to EtOH, however using the ethanolic mobile phase DMIVA and *S*-IVA co-eluted, therefore it was not suitable (Supplementary Information Figure S2). Addition of small amounts of ACN to MEOH as a secondary solvent, however, lead to reduced retention times without modifying the resolutions significantly (Supplementary Information Figure S3). Thus, this option was also evaluated during further method optimization.

3.2. Method optimization by experimental design

Conventional method optimization is usually performed by the so-called OFAT approach (one factor at a time), which leads to a multitude of experiments, whilst gaining only little knowledge about the process itself. Due to these shortcomings, experimental design-based, multivariate optimization of analytical techniques have become widespread in recent years. The main advantage of this approach is that it offers maximum process understanding with a minimal number of experiments [22,23].

Thus, a multivariate methodology was undertaken for a rapid optimization of numerous parameters affecting the simultaneous separation of the analytes. Based on the preliminary experimental runs, four critical quality attributes were selected and monitored as responses in the experimental runs. These included: R_s between DHIVA and DMIVA (abbreviated R_{s1}), R_s between DMIVA and *R*-IVA (R_{s2}), R_s between *R*-IVA and *S*-IVA (R_{s3}) and total analysis time (measured as retention time of *S*-IVA, $t_{r,S\text{-IVA}}$). Critical process parameters were identified based on our previous experience with polar organic mode on polysaccharide-type CSPs and a risk assessment of different factors that could influence the performance of the method. The critical process parameters selected as experimental variables during the DoE runs were defined as DEA volume ratio added to the mobile phase (DEA%, range 0.05% – 0.15%), ACN/MeOH volume ratio of the mobile phase (ACN%, 0–10%), flow rate (0.3 – 0.7 mL/min) and column temperature (T, 10–40 °C). In our work DEA was used as modifier however the nature of the basic and/or acidic modifier may deeply influence the separation [15].

In order to obtain thorough information about the influence of defined factors on selected responses and thereby to achieve the optimal chromatographic conditions, aiming to fulfil all response target settings, a full factorial experimental design with three center points was selected.

The design returned a total of 19 experimental runs, including three replicate center pointed experiments. The sample consisted of 8000 μg/mL *S*-IVA and 80 μg/mL of each impurity (impurity

Table 2
Optimized method conditions with predicted and experimentally obtained response values.

Optimized method conditions					R_{s1}	R_{s2}	R_{s3}	$t_{r,S\text{-IVA}}$
DEA%	ACN%	Flow rate (ml/min)	T (°C)	Predicted values	2.02 (1.85 – 2.19)	1.58 (1.54 – 1.62)	2.00 (1.95 – 2.05)	23.71 (21.98 – 25.57)
0.06	2	0.45	12	Experimental obtained values	2.13	1.55	1.98	23.20

levels at 1.0% relative to *S*-IVA) in MeOH. All experimental runs were performed in triplicate and the average values were introduced in the worksheet. The design matrix and the recorded values for all responses are summarized in Supplementary Information Table S1. The obtained data was fitted by partial least squares (PLS) regression and the model passed the replicative plot analysis for all responses (Supplementary Information Figure S4), meaning that replicate errors did not interfere with data analysis. Histogram plots of responses indicated normal distribution for reponses R_{s1}, R_{s3}, but not for R_{s2} and $t_{r,S\text{-IVA}}$. For the latter two, the histograms showed strong positive skewness, implying that the frequency of lower values in the dataset was much higher. In order to achieve approximately normal distribution, logarithmic transformations were employed, which resulted in a substantial increase in model predictability (Q^2) for both responses. The model was further adjusted by deleting non-significant factors and adding detected square values to increase the Q^2 values. The final coefficient plots obtained, with the significant factors affecting each response are presented in Supplementary Information Figure S4. For all of monitored responses, the experimental variables ACN%, flow rate and *T* presented a negative correlation, indicating that an increase in any of these factors resulted in a decrease in all R_s values, but also a decrease in $t_{r,S\text{-IVA}}$. DEA% in most cases had no significant effect upon the responses, apart from R_{s2} where, in comparison to ACN%, flow rate and *T* also presents a significant inverse proportionality with the selected response, although being the least influential of the defined factors.

Further model refinement implied the appraisal of quadratic terms inside the model. The presence of quadratic terms indicates a non-linear relationship in-between factors and responses and suggests the existence of curvature inside the model. Quadratic terms were not identified in case of R_{s2} and R_{s3}. Regarding R_{s1} and $t_{r,\,S\text{-}IVA}$ significant quadratic terms were observed and included in the analysis of model performance indicators. As the refined model allows only one quadratic term to be included in the regression equation, this was fulfilled by selecting the one for which the corresponding singular factor has the greatest impact on the selected response. Hence, in case of R_{s1} and $t_{r,\,S\text{-}IVA}$, ACN% *x* ACN% and Flow *x* Flow were retained, respectively.

In all cases, significant regression models were obtained ($p < 0.05$) and apart from the case of $t_{r,S\text{-IVA}}$, no lack of fit was detected ($p > 0.05$). In the latter case, the lack of fit was also evident by the negative model validity value. In contrast to this, model reproducibility showed extremely high values (õ.99), since the replicate runs resulted in almost identical retention times of the main peak (see Supplementary Information Table S1). Although retention time reproducibility is desirable and mostly expected in chromatographic techniques, this also means, that the pure error inside the model tends to zero and thus, the low model validity in case of $t_{r,\,S\text{-}IVA}$ can be explained by high reproducibility. The method was subsequently optimized using the prediction spreadsheet function of the software, applying the following criteria: all R_s values maximized, with a critical minimal value ≤ 1.5, and $t_{r,S\text{-IVA}}$ minimized.

The optimizer set point results obtained after the performed experiments during screening is based on a Monte Carlo simulation, where parameter settings were chosen according to the lowest log(D) value, with DEA = 0.058%, ACN = 1.68%, flow rate =0.46 mL/min and column temperature = 12.0 °C. Design space was evaluated around the aforementioned parameter settings. The 4D design space explorer map (Supplementary Information Figure S5) indicates that the chromatographic system returns optimal results only at low column temperature and flow rate settings. At the lowest set points of both the flow rate and column temperature, the proportion of ACN is allowed to be used in a wider range, showing a shift towards tighter specification limits as higher settings for both flow rate and column temperature are required. The set point analysis function of the software revealed that the frequency histograms of the selected factors and defined responses follow a normal distribution (Supplementary Information Figure S6 and S7), and the individual probability of failure for the defined responses is situated below 1%, with an overall probability of failure of 1.7%. For ease of use, the final proposed method uses slightly different parameter settings (most parameter settings are rounded), which still lie inside the design space and return satisfactory results in terms of selected response requirements. Table 2 shows the optimized parameters of the chromatographic system and the closeness of the predicted and experimentally obtained values for all responses, using the recommended settings. Since the analytical target profile of the method was fulfilled, further method optimization was not undertaken. The parameters of the final method were the following Lux Cellulose-2 column with 0.06% (v/v) DEA in MeOH/ACN 98/2 (v/v) with 0.45 mL/min flow rate at 12 °C.

3.3. Method validation and application

Validation of the optimized method was performed according to International Council for Harmonization guideline Q2 (R1) for all related substances and for *R*-IVA as chiral impurity, with respect of sensitivity, linearity, accuracy, and precision [24]. The limit of detection (LOD) and the limit of quantification (LOQ) were calculated based on signal-to-noise ratios of 3:1 and 10:1 for the LOD and LOQ, respectively. (Baseline noise was measured considering a peak to peak within 3 min selected in three different parts of the chromatogram of the standard solution.) The obtained values are summarized in Table 3. Based on the results, the linearity of the method was evaluated at eight concentration levels for all impurities and calibration plots were represented by plotting peak areas against corresponding concentrations (expressed in μg/mL). The correlation coefficient was determined by linear least squares regression analysis and it is higher than 0.9972 in all cases. Moreover, for all impurities 95% confidence intervals of the y-intercepts included zero and random distribution of the residuals was observed.

The accuracy and precision were analyzed by performing intra- (repeatability) and inter-day evaluation (two consecutive days) of three concentration levels for all impurities, covering the linearity range, each solution being injected five times. The accuracy (expressed in mean recovery%) ranged from 97.52% to 104.32%. The repeatability (expressed as RSD%) determined by five parallel injections of the solutions on the same day was between 0.41% and 2.29%. Intermediate precision of the method (expressed in RSD%) was investigated on two consecutive days and was lower than 3.56%.

Table 3
Assay validation data.

Parameter	Level	IMP-1	IMP-2	DHIVA	DMIVA	*R*-IVA
Range (μg/mL)		2 – 80	2 – 80	2.7 – 64	2.7 – 64	4 – 80
Range (%)		0.025% - 1%	0.025% - 1%	0.034% - 0.8%	0.034% - 0.8%	0.05% - 1%
r^2		0.9992	0.9989	0.9980	0.9997	0.9972
LOD (μg/mL)		0.12	0.12	0.81	0.60	1.20
LOQ (μg/mL)		0.40	0.40	2.70	2.0	4.0
Accuracy (%)						
	I*	98.90 ± 0.90	104.32 ± 1.01	99.69 ± 1.03	103.92 ± 1.45	103.45 ± 1.19
	II**	97.52 ± 1.12	99.55 ± 2.21	102.65 ± 0.99	97.91 ± 0.75	98.94 ± 0.67
	III***	98.29 ± 0.22	101.81 ± 0.88	103.51 ± 0.75	99.81 ± 0.19	98.62 ± 0.34
Content repeatability (RSD)						
	I*	1.95	1.53	2.29	1.50	0.63
	II**	0.68	0.55	1.19	1.02	0.97
	III***	0.41	0.56	0.55	0.49	0.66
Content precision (RSD)						
	I*	2.12	1.74	3.56	1.69	1.11
	II**	0.69	0.38	1.26	1.09	1.01
	III***	0.82	0.49	0.81	1.52	2.27

* Level I: IMP-1 = 4 μg/ml, IMP-2 = 4 μg/ml, DHIVA = 4 μg/ml, DMIVA = 5.4 μg/ml, *R*-IVA = 8 μg/ml.
** Level II: IMP-1 = 16 μg/ml, IMP-2 = 16 μg/ml, DHIVA = 12 μg/ml, DMIVA = 10.8 μg/ml, *R*-IVA = 16 μg/ml.
*** Level III: IMP-1 = 56 μg/ml, IMP-2 = 56 μg/ml, DHIVA = 40 μg/ml, DMIVA = 54 μg/ml, *R*-IVA = 56 μg/ml.

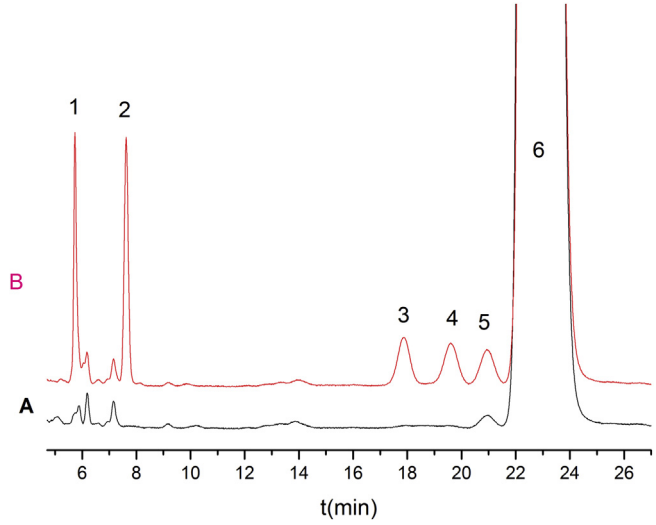

Fig. 3. Chromatograms of (A) Solution of Ivabradine 5 mg tablet. (B) Solution of Ivabradine 5 mg film-coated tablet spiked with all impurities at the 0.05% level. Experimental conditions: Lux Cellulose-2 column with 0.06% (v/v) DEA in MeOH/ACN 98/2 (v/v) with 0.45 mL/min flow rate at 12 °C. 1. IMP-1, 2. IMP-2, 3. DHIVA, 4. DMIVA, 5. *R*-IVA, 6. *S*-IVA.

Based on the obtained results the optimized method proved to be sensitive, linear, accurate and precise for the determination of five different impurities, including *R*-IVA as chiral impurity.

The optimized and validated method was applied to the analysis of real samples, in the form of film-coated tablets with a nominal content of 5 mg *S*-IVA base. The representative chromatograms recorded for the sample solution and the sample solution spiked with impurities are shown in Fig. 3A and B, respectively. Only *R*-IVA of the monitored impurities could be quantified in the commercial tablet, the other impurities were below (or close) the LOD. The content of *R*-IVA was 0.032 ± 0.001%. In addition to the known related substances, minor unidentified peaks could also be observed in the sample chromatogram, which could be indicating unknown impurities or may be the results of different exicipients used in the tablet formulation. Using peak normalization at 286 nm, the sum of the total impurities was calculated as 0.14 ± 0.01%.

4. Concluding remarks

A novel, single HPLC method using Lux Cellulose-2 column in polar organic mode was developed using DoE for the simultaneous determination of DHIVA, DMIVA, IMP-1 and IMP-2 as related substances as well as *R*-IVA as enantiomeric impurity in *S*-IVA. The method was validated according to the International Council for Harmonization guideline Q2(R1) and proved to be precise and accurate for determination of at least 0.05% or below for all impurities in *S*-IVA samples. Application of the method was tested on a commercial tablet and showed that the tablet contains *R*-IVA impurity, but below 0.05%. Our method could be applied in an industrial environment for simultaneous quantification of chemical and chiral related substances of *S*-IVA in one run to save time and money. Furthermore, the present method is another example that related substances and enantiomeric impurities can be determined by a single method using polysaccharide-type CSP in polar organic mode.

Acknowledgements

This work was supported by the János Bolyai Research Scholarship of the Hungarian Academy of Sciences and by the Semmelweis Innovation Found STIA-M-17 and STIA-18-KF (to G. Tóth). The financial support from Bolyai + New National Excellence Program (grant number: UNKP-19-4-SE-28) of the Ministry of Human Capacities is highly appreciated (G.Tóth).

Appendix A. Supplementary data

Supplementary material related to this article can be found, in the online version, at doi:https://doi.org/10.1016/j.jpba.2019.112851.

References

[1] K. Swedberg, M. Komajda, M. Böhm, J.S. Borer, I. Ford, A. Dubost-Brama, G. Lerebours, L. Tavazzi, Ivabradine and outcomes in chronic heart failure (SHIFT): a randomised placebo-controlled study, Lancet 376 (2010) 875–885, http://dx.doi.org/10.1016/S0140-6736(10)61198-1.
[2] C.W. Yancy, M. Jessup, B. Bozkurt, J. Butler, D.E. Casey, M.M. Colvin, M.H. Drazner, G. Filippatos, G.C. Fonarow, M.M. Givertz, S.M. Hollenberg, J. Lindenfeld, F.A. Masoudi, P.E. McBride, P.N. Peterson, L.W. Stevenson, C.

Westlake, C. Westlake, ACC/AHA/HFSA focused update on new pharmacological therapy for heart failure: an update of the 2013 ACCF/AHA guideline for the management of heart failure: a report of the american college of Cardiology/American heart association task force on clinical practice guidelines and the heart failure society of america, Circulation 134 (2016) (2016), http://dx.doi.org/10.1161/CIR.0000000000000435.
[3] C. Thollon, J.P. Bidouard, C. Cambarrat, L. Lesage, H. Reure, I. Delescluse, J. Vian, J.L. Peglion, J.P. Vilaine, Stereospecific *in vitro* and *in vivo* effects of the new sinus node inhibitor (+)-S 16257, Eur. J. Pharmacol. 339 (1997) 43–51, http://dx.doi.org/10.1016/S0014-2999(97)01364-2.
[4] J.P. Vilaine, C. Thollon, N. Villeneuve, J.L. Peglion, Procoralan, a new selective I f current inhibitor 5 (2003) G26–G36, http://dx.doi.org/10.1016/S1520-765X(03)90005-8.
[5] chiraltech.com/wp-content/uploads/2017/04/Ivabradine-CHIRALPAK-IG.pdf (accessed 08.29.2019).
[6] P. Pikul, M. Jamrógiewicz, J. Nowakowska, W. Hewelt-Belka, K. Ciura, Forced degradation studies of Ivabradine and in silico toxicology predictions for its new designated impurities, Front. Pharmacol. 7 (2016), http://dx.doi.org/10.3389/fphar.2016.00117.
[7] P.N. Patel, R.M. Borkar, P.D. Kalariya, R.P. Gangwal, A.T. Sangamwar, G. Samanthula, S. Ragampeta, Characterization of degradation products of Ivabradine by LC-HR-MS/MS: a typical case of exhibition of different degradation behaviour in HCl and H_2SO_4 acid hydrolysis, J. Mass Spectrom. 50 (2015) 344–353, http://dx.doi.org/10.1002/jms.3533.
[8] S. Maheshwari, A. Khandhar, A.J.-E.J. of, undefined, Quantitative determination and validation of ivabradine HCl by stability indicating RP-HPLC method and spectrophotometric method in solid dosage form, Eurasian, J. Anal. Chem. 5 (2010) (2010) 53–62.
[9] N.P. Nadella, V.N. Ratnakaram, N. Srinivasu, Development and validation of UPLC method for simultaneous quantification of carvedilol and ivabradine in the presence of degradation products using DoE concept, J. Liq. Chromatogr. Relat. Technol. 41 (2018) 143–153, http://dx.doi.org/10.1080/10826076.2018.1427595.
[10] T. Ikai, Y. Okamoto, Structure Control of Polysaccharide Derivatives for Efficient Separation of Enantiomers by Chromatography, Chem. Rev. 109 (2009) 6077–6101, http://dx.doi.org/10.1021/cr8005558.
[11] B. Chankvetadze, Polysaccharide-Based Chiral Stationary Phases for Enantioseparations by High-Performance Liquid Chromatography: An Overview, 2019, pp. 93–126, http://dx.doi.org/10.1007/978-1-4939-9438-0_6.
[12] H. Ates, A.A. Younes, D. Mangelings, Y. Vander Heyden, Enantioselectivity of polysaccharide-based chiral selectors in polar organic solvents chromatography: implementation of chlorinated selectors in a separation strategy, J. Pharm. Biomed. Anal. 74 (2013) 1–13, http://dx.doi.org/10.1016/j.jpba.2012.09.025.
[13] E.P. Sousa, M.E. Tiritan, R.V. Oliveira, C.M.M. Afonso, Q.B. Cass, M.M.M. Pinto, Enantiomeric resolution of kielcorin derivatives by HPLC on polysaccharide stationary phases using multimodal elution, Chirality 16 (2004) 279–285, http://dx.doi.org/10.1002/chir.20031.
[14] S. Niedermeier, I. Matarashvili, B. Chankvetadze, G.K.E. Scriba, Simultaneous determination of dextromepromazine and related substances 2-methoxyphenothiazine and levomepromazine sulfoxide in levomepromazine on a cellulose tris(4-methylbenzoate) chiral column, J. Pharm. Biomed. Anal. 158 (2018) 294–299, http://dx.doi.org/10.1016/j.jpba.2018.06.012.
[15] L. Mosiashvili, L. Chankvetadze, T. Farkas, B. Chankvetadze, On the effect of basic and acidic additives on the separation of the enantiomers of some basic drugs with polysaccharide-based chiral selectors and polar organic mobile phases, J. Chromatogr. A 1317 (2013) 167–174, http://dx.doi.org/10.1016/j.chroma.2013.08.029.
[16] A.C. Servais, B. Janicot, A. Takam, J. Crommen, M. Fillet, Liquid chromatography separation of the chiral prodrug eslicarbazepine acetate and its main metabolites in polar organic mode. Application to their analysis after in vitro metabolism, J. Chromatogr. A 1467 (2016) 306–311, http://dx.doi.org/10.1016/j.chroma.2016.07.022.
[17] R. Ferretti, L. Zanitti, A. Casulli, R. Cirilli, Unusual retention behavior of omeprazole and its chiral impurities B and E on the amylose tris (3-chloro-5-methylphenylcarbamate) chiral stationary phase in polar organic mode, J. Pharm. Anal. 8 (2018) 234–239, http://dx.doi.org/10.1016/j.jpha.2018.04.001.
[18] M. Foroughbakhshfasaei, Z.-I. Szabó, G. Tóth, Validated LC method for determination of enantiomeric purity of apremilast using polysaccharide-type stationary phases in polar organic mode, Chromatographia 81 (2018) 1613–1621, http://dx.doi.org/10.1007/s10337-018-3546-9.
[19] Z.-I. Szabó, M. Foroughbakhshfasaei, R. Gál, P. Horváth, B. Komjáti, B. Noszál, G. Tóth, Chiral separation of lenalidomide by liquid chromatography on polysaccharide-type stationary phases and by capillary electrophoresis using cyclodextrin selectors, J. Sep. Sci. 41 (2018) 1414–1423, http://dx.doi.org/10.1002/jssc.201701211.
[20] Z.-I. Szabó, M. Foroughbakhshfasaei, B. Noszál, G. Tóth, Enantioseparation of racecadotril using polysaccharide-type chiral stationary phases in polar organic mode, Chirality 30 (2018) 95–105, http://dx.doi.org/10.1002/chir.22772.
[21] M. Foroughbakhshfasaei, Z.-I. Szabó, A. Mirzahosseini, P. Horváth, G. Tóth, Enantiomeric quality control of *R* -Tofisopam by HPLC using polysaccharide-type chiral stationary phases in polar organic mode, Electrophoresis 39 (2018) 2566–2574, http://dx.doi.org/10.1002/elps.201800220.
[22] S. Orlandini, S. Pinzauti, S. Furlanetto, Application of quality by design to the development of analytical separation methods, Anal. Bioanal. Chem. 405 (2013) 443–450, http://dx.doi.org/10.1007/s00216-012-6302-2.
[23] P.K. Sahu, N.R. Ramisetti, T. Cecchi, S. Swain, C.S. Patro, J. Panda, An overview of experimental designs in HPLC method development and validation, J. Pharm. Biomed. Anal. 147 (2018) 590–611, http://dx.doi.org/10.1016/J.JPBA.2017.05.006.
[24] International Council for Harmonization Guideline Q2(R1), Validation of Analytical Procedures: Text and Methodology, 2005 (Accessed 08.29.2019) https://www.ich.org/fileadmin/Public_Web_Site/ICH_Products/Guidelines/Quality/Q2_R1/Step4/Q2_R1__Guideline.pdf.